Korean J. Chem. Eng., 34(6), 1781-1785 (2017)
DOI: 10.1007/s11814-017-0087-0

pISSN: 0256-1115
eISSN: 1975-7220

Phase behavior of arbutin/ethanol/supercritical CO_2 at elevated pressures

Chang-Nam Han* and Choon-Hyoung Kang,†**

*Department of Advanced Chemical Engineering, Chonnam National University, Gwangju 61186, Korea
**Department of Chemical Engineering, Chonnam National University, Gwangju 61186, Korea
(*Received 10 January 2017 • accepted 20 March 2017*)

Abstract−The phase behavior of a ternary system containing arbutin, which is effective for skin lightening, in a solvent mixture of ethanol and supercritical carbon dioxide (CO_2) was investigated. A high-pressure phase equilibrium apparatus equipped with a variable-volume view cell was used to measure the phase equilibrium loci of the ethanol+CO_2 binary mixture from 298.2 K to 313.2 K and pressures between 2 MPa and 9 MPa. The solubility of arbutin in the mixed solvent comprising ethanol and CO_2, which equivalently represents the critical locus of T-x, was determined as a function of temperature, pressure, and solvent composition by measuring the cloud points under various conditions. Throughout, the arbutin loading was maintained at 1.5 wt% on a CO_2-free basis in the solvent mixture and the pressure and temperature were varied up to 14 MPa and 334 K, respectively. For a CO_2 loading less than 34 wt% on ethanol basis, the cloud point was not observed. However, the solid remained undissolved when the CO_2 loading exceeded 54 wt%. Between these loadings, steep and almost pressure-insensitive solubility curves, which extended downward to the vaporization boundary, were found.

Keywords: Arbutin, Supercritical CO_2, Cloud Point, Solubility, Mixed Solvent

INTRODUCTION

Hydroquinone, kojic acid, azelaic acid (a corticosteroid), and retinoic acid have been used individually or in combination for the treatment of the skin diseases resulting from the excess deposition of the melanotic pigment. Among these, the hydroquinone formulation is the most common and is reportedly effective in about 80% of the patients. However, the formulation is known to be unstable and to induce skin irritation. Furthermore, it may cause dermatitis when used repetitively. Hyperpigmentation occurs following inflammation, with side effects including permanent bleaching due to cytotoxins, ochronosis [1-3], etc. Arbutin (hydroquinone-β-D-glucopyranoside), a combined derivative of hydroquinone and glucopyranoside, is presented as a therapeutic agent for skin diseases caused by the excess deposition of the melanotic pigment [4,5].

In general, the biological activity of a drug is highly dependent on the size, size distribution, and morphology of the drug particles. This fact has given rise to the concern about effective micronization technologies [6,7]. Micronization is one of the core technologies used in the food, polymer, and fine chemical industries as well as in the fields of materials science, medicine, etc. The commonly used particle size controlling techniques are crushing, grinding, ball milling, spray drying, solution subsidence, and crystallization. A recrystallization process using a supercritical fluid such as CO_2 was proposed for the preparation of size- and shape-regulated particles.

In general, a supercritical fluid exhibits rapid mass and heat transfer, outstanding dissolving capacity, and high penetrability in micropores due to its low viscosity and high diffusivity coefficient. Among the various existing processes such as reaction and decomposition, extraction, distillation, crystallization, absorption, adsorption, drying, and cleaning, supercritical fluid crystallization has come into the spotlight as an innovative technique that can help resolve the issues associated with the other techniques, including low efficiency, low quality, low speed, and adverse environmental effects [8].

In the SAS (Supercritical fluid as anti-solvent) process, a solution of the solute particles in a good solvent is exposed to a supercritical fluid acting as an anti-solvent. This results in a drastic deterioration of the solubility, followed by the segregation of the solute [9,10]. The size and shape of the resulting particles are highly dependent on the operation conditions of the recrystallization process. Therefore, knowledge of the phase behavior of the mixture is a requisite for achieving control over the morphological characteristics of the particles, which in turn determines the biological activity if the mixture is intended for use as a drug. Depending on the operating methods, the process is classified as GAS (Gas anti-solvent), ASES (Aerosol solvent extraction sSystem), and SEDS (Solution enhanced dispersion by supercritical fluid) [11]. In the ASES process, the solution is dispersed in a vessel filled with a supercritical fluid, which is consecutively sprayed into a crystallization vessel at high pressure through a nozzle. Owing to the instantaneous buildup of supersaturation at levels exceeding those in the GAS process, the resulting particles are expected to be very small with a narrow size distribution. Thus, small and relatively uniform particle sizes would be observed.

Because of its low critical temperature (31.1 °C) and critical pres-

†To whom correspondence should be addressed.
E-mail: chkang@chonnam.ac.kr

sure (7.38 MPa), CO_2 is a suitable supercritical solvent for processes involving with materials that cannot sustain thermal surges. The nontoxicity, nonflammability, low cost, and reusability of CO_2 facilitate its use in the manufacture of microparticles intended for a drug and/or its delivery system.

In this research, the phase behavior of a mixture that is obligatorily required to determine the operating conditions of the arbutin micronization process was measured using a high-pressure phase equilibrium apparatus equipped with a variable-volume view cell. First, the phase behavior of the binary mixed solvent consisting of ethanol and supercritical CO_2 was measured. This was followed by correlation of the experimental phase behavior data with the Peng-Robinson equation of state for satisfactory accuracy and the determination of the interaction parameters of the mixture [12]. In addition, the phase behavior of the ternary system including arbutin in the mixed solvent was measured, and the range of operating conditions for arbutin micronization was proposed on the basis of the previously presented findings. The operating conditions proposed in this work were also realized through the subsequent experiments on arbutin particle preparation conducted in our lab [13].

EXPERIMENTAL

1. Materials

Arbutin (mass fraction purity>0.98) and ethanol (mass fraction purity>0.999) for dissolving arbutin were obtained from Sigma and Daejung Chemicals & Metals Co., Ltd., respectively. CO_2 (mass fraction purity>0.9999) was provided by Daechang Gas, Korea. The chemicals were used without further purification. The properties of ethanol and CO_2 are summarized in Table 1.

2. Apparatus and Procedure

A high-pressure phase equilibrium apparatus equipped with a variable-volume view cell was used to measure the high-pressure phase behavior, as shown in Fig. 1. The measurement range of this apparatus was up to 80 °C and 300 bar at NTP. The conditions of the cell were manipulated using a pressure generator (High-Pressure Equipment Co, 62-6-10 model). A borescope illuminated by a light source was used to observe the sample behavior in the cell. The image observed through the sapphire window was transmitted to a camera connected to a PC. The cell was sealed using the O-ring of the Viton material, and the sample in the cell was stirred with a magnetic bar driven by a permanent magnet from outside the cell. The cell was placed in an air bath (Han Beak Scientific Co.), whose temperature was controlled within ±0.1 °C. The temperatures of the interior and the wall of the cell were measured using precision thermometers (Hart scientific Co, 1502A model).

Table 1. Physical properties and acentric factors for CO_2 and ethanol used in this work [16]

Component	CO_2	Ethanol
M.W.	44.01	46.07
T_b (K)	195.0	351.4
T_c (K)	304.1	513.9
P_c (MPa)	7.38	6.14
Acentric factor	0.225	0.644

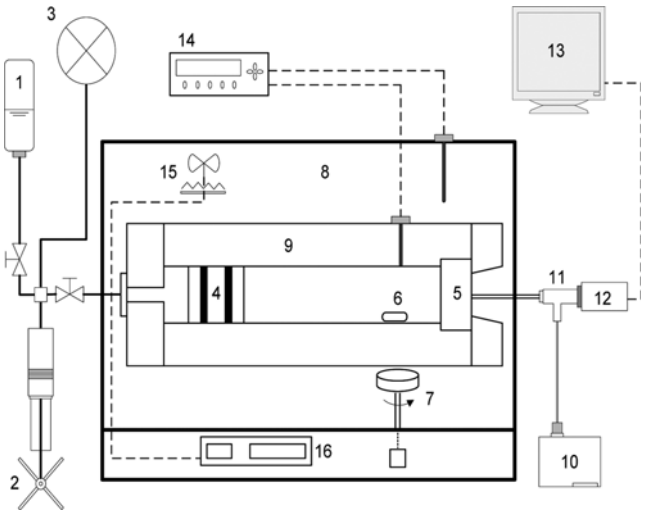

Fig. 1. Schematic of the experimental apparatus.

1. Water	9. Variable-volume cell
2. Pressure generator	10. Light source
3. Pressure gauge	11. Bore scope
4. Piston	12. Camera
5. Sapphire window	13. Monitor
6. Magnetic bar	14. Temperature indicator
7. Stirrer	15. Heater
8. Air bath	16. Heating controller

The pressure in the cell was measured using a precision pressure gauge (HEISE®, CM-130994 model), with a precision of 10 psi.

Before charging with the solution, the cell was flushed with CO_2 to remove any possible undesired materials such as air. The loading amount of the solution in the cell was calculated by measuring the weights of the syringe filled with the solution and the empty syringe after injecting the solution into the cell with an uncertainty of ±0.01 g.

At a prescribed temperature, the boiling point of the CO_2 and ethanol binary mixture was determined by observing the cloud point. To obtain the cloud point, the pressure was increased until a clear solution was observed. After the pressure was fixed, the temperature was carefully lowered until the cloud point was observed again. The cloud point is generally confirmed once the given solution becomes turbid and the solid is segregated. Thus, a mesophase is observed when the mixture becomes turbid upon the precipitation of the solute at the cloud point. The pressure and temperature at the cloud point mark the boundary beyond which the immiscibility region of the solution appears. That is, it is the solubility limit of the solute in the solvent [14,15].

The experiments were repeated at least three times, and the mean values were obtained.

RESULTS AND DISCUSSION

1. Phase Behavior of CO_2/Ethanol Binary System

The high-pressure gas-liquid equilibrium for the CO_2/ethanol binary mixture was determined by measuring the boiling point. The results are summarized in Table 2. In Figs. 2 and 3, the experimental results are shown in the form of the gas-liquid phase dia-

Table 2. Experimental vapor-liquid equilibrium data for the CO_2 (1)+ethanol (2) system

	Pressure (MPa)			
CO_2 mole fraction	298 K	303 K	308 K	313 K
0.973	6.30	6.98	7.68	8.38
0.948	6.10	6.71	7.40	8.29
0.875	5.71	6.29	7.01	7.83
0.765	5.52	6.05	6.83	7.50
0.626	4.90	5.62	6.41	7.22
0.463	3.98	4.62	5.49	6.28
0.246	2.31	2.66	3.11	3.82

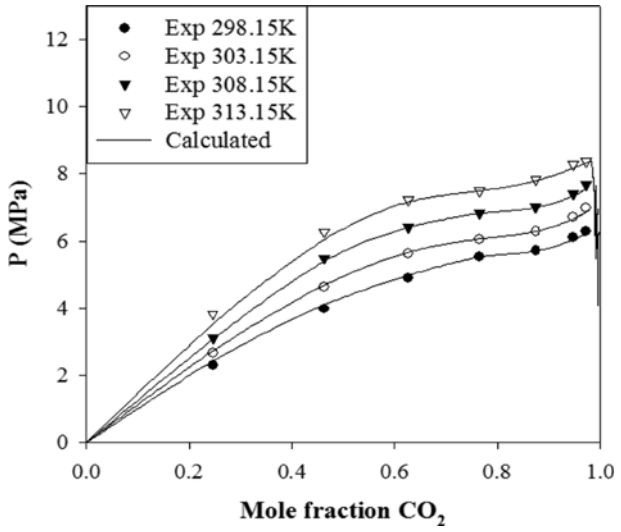

Fig. 2. Comparison of the measured data and correlations with the Peng-Robinson EOS (k_{ij}=0.057, η_{ij}=0.034).

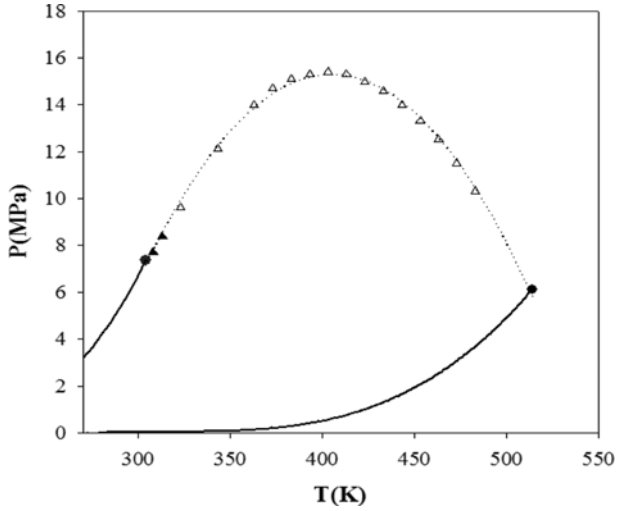

Fig. 3. P-T diagram of the CO_2+ethanol binary mixture. The experimental critical loci of this work are compared with the literature data (▲: the present work, △: Ziegler et al. [25], ---: sketched line, —: vapor pressure of pure components, and ●: critical points of pure components).

gram (P-x-y) and critical locus (P-T), respectively.

Using the Peng-Robinson EOS, the high-pressure gas-liquid phase equilibrium of CO_2 and ethanol was modeled.

$$P = \frac{RT}{V-b} - \frac{a}{V^2+2bV-b^2} \tag{1}$$

where P is the absolute pressure, T is the absolute temperature, R is the gas constant, and a and b are the energy and size parameters, respectively. According to the rule of mixture, a_{mix} and b_{mix} are calculated as follows [17-21].

$$a_{mix} = \sum_i \sum_j x_i x_j a_{ij} \tag{2}$$

$$a_{ij} = (a_{ii}a_{jj})^{0.5}(1-k_{ij}) \tag{3}$$

$$b_{mix} = \sum_i \sum_j x_i x_j b_{ij} \tag{4}$$

$$b_{ij} = [0.5(b_{ii}+b_{jj})](1-\eta_{ij}) \tag{5}$$

Though in theory, k_{ij} and η_{ij} represent the interaction between the comprising unlike molecules, it is common practice to determine these parameters through correlation with the experimental data. The parameters a_{ij} and b_{ij} pertain to the pure components. The properties including the acentric factor for the pure components considered in this study are listed in Table 1.

For modeling the experimental data, the objective function (OBF) shown in Eq. (6) was used. The correlation results were checked and validated using the root mean square error (RMSE) and average absolute deviation (AAD) percentages, defined in Eqs. (7) and (8), respectively [22-24].

$$OBF = \sum_{n=i}^{NDG} W_n \sum_{i=1}^{NP} \left[\left(\frac{T_{e,i} - T_{m,i}}{\sigma_{T,i}} \right)^2 + \left(\frac{P_{e,i} - P_{m,i}}{\sigma_{P,i}} \right)^2 + \sum_{i=1}^{NC-1} \left(\frac{x_{e,i,j} - x_{m,i,j}}{\sigma_{x,i,j}} \right)^2 + \sum_{i=1}^{NC-1} \left(\frac{y_{e,i,j} - y_{m,i,j}}{\sigma_{y,i,j}} \right)^2 \right] \tag{6}$$

$$RMSE(\%) = \left[\frac{1}{k} \sum_{i=1}^{k} \left(\frac{Z_i - ZM_i}{ZM_i} \right)^2 \right]^{1/2} \tag{7}$$

$$AAD(\%) = \frac{1}{k} \sum_{i=1}^{k} \left| \left(\frac{Z_i - ZM_i}{ZM_i} \right) \right| \tag{8}$$

NDG in Eq. (6) denotes the number of data groups used in the regression analysis, and w represents the mass of the n^{th} data group. NP represents the number of experimental data points and NC, the number of components. y and x refer to the mole fractions in the vapor and liquid phases, whereas e and m denote the measured and correlated data, respectively. σ represents the standard deviation. In Eqs. (7) and (8), Z denotes the calculated value and ZM stands for the value of the experimental data corresponding to Z. In addition, k denotes the number of data points.

The calculated and experimental values of the temperature, pressure, and mole fractions were compared. The correlation results favorably agreed with the experimental P-x envelopes, as shown in Fig. 2. The binary interaction parameters were found to be k_{ij}= 0.057 and η_{ij}=0.034. From the values of RMSE (%) and AAD (%)

Table 3. Correlation results for CO_2 (1)+ethanol (2) system with the Peng-Robinson EOS (see Eqs. (7) and (8) for the root mean square error (RMSE) and average absolute deviation (AAD), respectively)

RMSE (%)				
	298 K	303 K	308 K	313 K
Temperature	9.99	1.38	1.08	7.84
Pressure	4.12	0.73	0.59	7.37
Liq. CO_2	2.43	0.51	0.44	7.58
Liq. ethanol	6.79	1.92	1.76	14.81
AAD (%)				
	298 K	303 K	308 K	313 K
Temperature	7.66	1.02	0.76	4.33
Pressure	3.49	0.60	0.44	3.79
Liq. CO_2	1.85	0.30	0.32	3.79
Liq. ethanol	4.75	1.26	1.16	7.64

listed in Table 3, a satisfactory correlation was reconfirmed.

With an increase in pressure, the saturated liquid composition slightly increased. However, the corresponding saturated gas composition remained almost constant. Meanwhile, the critical point shifted to the higher pressure and lower concentration region with an increase in temperature. As shown in Fig. 3, the critical locus estimated for the ethanol/CO_2 mixture using the Peng-Robinson EOS was comparable with the experimentally determined boiling points. Furthermore, the locus presented a typical type-I behavior [16].

Table 4. Phase transition measurements for 1.5 wt% arbutin in ethanol

33 wt% CO_2		63.38 wt% CO_2	
T (K)	T (K)	T (K)	P (MPa)
L-VL		LS-VLS	
294.8	3.585	296.8	5.171
305.6	4.551	304.5	6.137
314.5	5.309	311.7	7.102
321.5	5.861	317.7	7.929
327.8	6.412	326.6	8.964
333.0	6.826	333.4	10.00
41 wt% CO_2		54.13 wt% CO_2	
T (K)	T (K)	T (K)	P (MPa)
L-VL		L-VL	
293.7	3.792	293.9	4.482
302.9	4.896	300.7	5.378
LS-VLS		LS-VLS	
311.1	5.654	307.5	6.343
321.2	6.55	311.2	6.688
327.5	7.171	319.4	7.585
333.4	7.585	326.5	8.274
		333.0	8.964
L-LS		L-LS	
303.0	6.895	303.2	7.240
302.2	10.343	301.4	10.343
302.7	13.790	301.0	13.790

2. Phase Behavior of CO_2/Ethanol/Arbutin Ternary System

The cloud point and boiling point of the ternary system comprising arbutin in the mixed solvent of CO_2 and ethanol were measured. Arbutin loading was maintained at 1.5 wt% on ethanol basis in the solvent mixture throughout this study. The pressure and temperature were varied up to 14 MPa and 334 K, respectively. In the experiments, the CO_2 concentration in the mixture was varied from 33 wt% to 63.38 wt%.

For a CO_2 loading less than 34 wt% on ethanol basis, a cloud point was not observed, while the solid remained undissolved when the loading exceeded 54 wt%. Between these loadings, steep and almost pressure-insensitive solubility curves with a slight negative slope, which extended downward to the vaporization boundary, were found. The experimental results are summarized in Table 4, and the phase behavior of the mixture is shown in the form of a P-T diagram in Fig. 4. The fact that a small variation in temperature resulted in a drastic change in the solubility curve entailed experimental difficulties in determining the solubility curve.

In Fig. 4, the VLS-LS and VL-L lines show the boiling point of the mixture. For the mixture, the L-LS line represents the cloud point, which is equivalent to the solubility curve of the mixture. Only a single phase existed in the region to the right of the solubility curve, while segregated particles appeared and liquid coexisted with solid in the region to the left of the curve. As mentioned, the cloud point represents the solubility limit of the solute in the CO_2/ethanol mixed solvent at the given temperature and pressure. The locus of the cloud point formed the curve of the upper critical solution temperature (UCST) [14,15,26].

The study of the phase behavior of the binary and ternary systems helped us to determine the operating conditions of the SAS

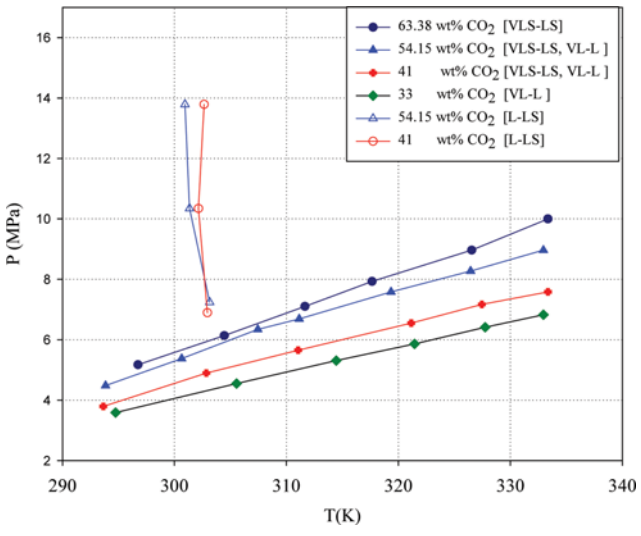

Fig. 4. The isopleths of the system of arbutin/ethanol/CO_2 at different concentrations of CO_2. Arbutin concentration on a CO_2-free basis is 1.5 wt%.

process for arbutin particles intended for use as a drug and/or its delivery system. For the SAS process to be feasible for arbutin particles, a pressure greater than 9 MPa and a CO_2 concentration over 64% should be maintained. On the other hand, the pressure limit, which is a minimum value to induce the phase split for the particle formation, slowly increased with the temperature. These results were realized in the subsequent experiments for arbutin particle preparation conducted in our laboratory [13].

CONCLUSIONS

The solubility of arbutin in a mixed solvent of supercritical carbon dioxide and ethanol was experimentally determined by using a high-pressure phase equilibrium apparatus equipped with a variable-volume view cell. The P-T curve for the binary system of carbon dioxide and ethanol was observed and it was confirmed that the binary mixture showed typical type I behavior. As the temperature increased, the critical point shifted to the higher pressure and the lower concentration region. The experimental P-x envelopes were correlated by using the Peng-Robinson equation of state in a satisfactory manner to obtain the parameters with k_{ij}=0.057 and η_{ij}=0.034. The critical locus of T-x was also determined.

The cloud point was determined by a function of temperature, pressure and composition of the ternary system of arbutin and the mixed solvent of ethanol and supercritical carbon dioxide. For the mixture, the L-LS line represents the solubility limit of arbutin in the mixed solvent. For CO_2 loading between 34 wt% and 54 wt% on the basis of ethanol, steep and thus very pressure-insensitive solubility curves, which extended downward to a vaporization boundary, were found.

On the basis of the results of the phase behavior study for the constituent binary and ternary systems, the possible operating condition for the SAS process for the arbutin particles preparation was proposed: In the particle preparation process, pressure greater than 9 MPa and the carbon dioxide concentration of over 64% should be maintained. In fact, these results were realized in our subsequent study of particle preparation [13].

ACKNOWLEDGEMENT

This work was supported by a grant (16IFIP-B089065-03) from Industrial Facilities & Infrastructure Research Program (IFIP) funded by Ministry of Land, Infrastructure and Transport of the Korean government.

REFERENCES

1. P. E. Engasser and H. I. Maibach, *J. Am. Acad. Dermatol.*, **5**, 143 (1981).
2. G. H. Findley, J. G. L. Morrison and I. W. Simon, *Br. J. Dermatol.*, **93**, 613 (1975).
3. J.-H. Paik and M.-H. Lee, *Korean J. Dermatol.*, **38**, 1303 (2000).
4. K. Maeda and M. Fukuda, *J. Pharm. Exp. Therap.*, **276**, 765 (1996).
5. A. E. Oliver, L. M. Crowe, P. S. Araujo, de E. Fisk and J. H. Crowe, *Biochim. Biophys. Acta*, **1302**, 69 (1996).
6. A. Martin and M. J. Cocero, *Adv. Drug Delivery Rev.*, **60,** 339 (2008).
7. V. J. Krukonis, *Supercritical Fluid Nucleation of Difficult-to-Comminute Solids*, Paper presented at the AIChE Annual Meeting, San Francisco, CA (1984).
8. M. E. Paulaitis, J. M. L. Penninger, R. D. Gray and P. Davidson Eds. *Chemical Engineering at Supercritical Fluid Condition*, Ann Arbor Science, Ann Arbor (1983).
9. P. M. Gallagher, M. P. Coffey, V. J. Krukonis, N. K. Klasutis, P. J. Johnston and M. L. Penninger, *Supercritical Fluid Science and Technology,* ACS Symposium Series 406, ACS, Washington D.C. (1989).
10. D.-Y. Kang, B.-J. Min, S.-G. Rho and C.-H. Kang, *Korean Chem. Eng. Res.*, **46**, 958 (2008).
11. B. Masoud and R. Sima, *J. Supercrit. Fluids*, **40**, 263 (2007).
12. D. Y. Peng and D. R. Robinson, *Ind. Eng. Chem. Fundam.*, **15**, 59 (1976).
13. B. E. Poling, J. M. Prausnitz and J. P. O'Connel, *The Properties of Gases and Liquids*, 5th Ed., McGraw-Hill, New York (2001).
14. Y.-S. Jang, Y. S. Choi and H.-S. Byun, *Korean J. Chem. Eng.*, **32**, 958 (2015).
15. Y.-S. Choi, S.-W. Chio and H. S. Byun, *Korean J. Chem. Eng.*, **33**, 277 (2016).
16. C.-N. Han and C.-H. Kang, *J. Nanosci. Nanotechnol.*, **16**, 6936 (2016).
17. P. H. van Konynenburg and R. L. Scott, *Philos. Trans. Royal Soc. London Ser. A*, **298**, 495 (1980).
18. M. A. McHugh and V. J. Krukonis, *Supercritical Fluid Extraction: Principles and Practice*, 2nd Ed., Butterworth-Heinemann, Boston (1994).
19. H.-S. Byun, C.-H. Kim and C. Kwak, *Korean Chem. Eng. Res.*, **30,** 387 (1992).
20. J. M. Prausnitz, R. N. Lichtenthaler and E. G. de Azervedo, *Molecular Thermodynamics of Fluid Phase Equilibria*, 2nd Ed., Prentice-Hall Inc., New Jersey (1987).
21. J.-U. Lee and G.-Y. Chung, *J. Korean Ind. Eng. Chem.*, **6**, 819 (1995).
22. H.-S. Byun and K.-P. Yoo, *Fluid Phase Equil.*, **249**, 55 (2006).
23. J. A. Baker, *Aust. J. Chem.*, **6**, 207 (1953).
24. Aspen Plus® User Guide, Version 12.1 (2003).
25. J. W. Ziegler, T. L. Chester, D. P. Innis, S. H. Page and J. G. Dorsey, in *Innovations in supercritical fluids. science and technology,* K. W. Hutchenson and N. R. Foster Eds., American Chemical Society, Washington, D.C. (1995).
26. F. P. Lucien and N. R. Foster, *J. Supercrit. Fluids*, **17**, 111 (2000).